Supporting Information

Rational design of N-doped C-encapsulated flower-like Nickel-based heterostructure microspheres anode toward high-capacity and stable lithium storage

Zhicheng Yu,[a] Shahriman Zainal Abidin,*[a] Natrina Mariane P. Toyong,[a] and Xiaojun Zhao*[b]

[a]College of Creative Arts, Universiti Teknologi MARA 40450 Shah Alam, Selangor Darul Ehsan, Malaysia. E-mail: shahriman.z.a@uitm.edu.my

[b]School of Metallurgical Engineering, Xi'an University of Architecture and Technology, Xi'an 710055, P. R. China (x.j.zhao@hotmail.com; xjzhao@xauat.edu.cn).
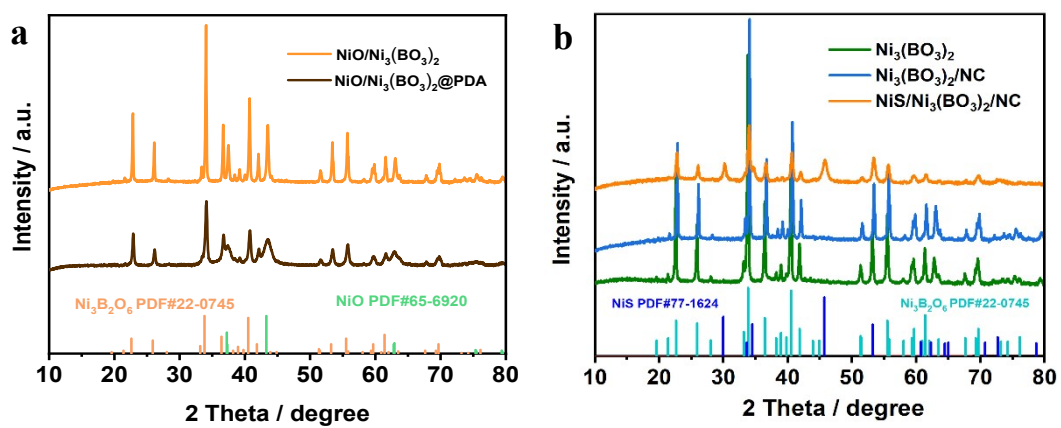
Fig. S1. XRD patterns of (a) NiO/Ni$_3$(BO$_3$)$_2$ and NiO/Ni$_3$(BO$_3$)$_2$/PDA, and (b) Ni$_3$(BO$_3$)$_2$, Ni$_3$(BO$_3$)$_2$/NC, and NiS/Ni$_3$(BO$_3$)$_2$/NC.
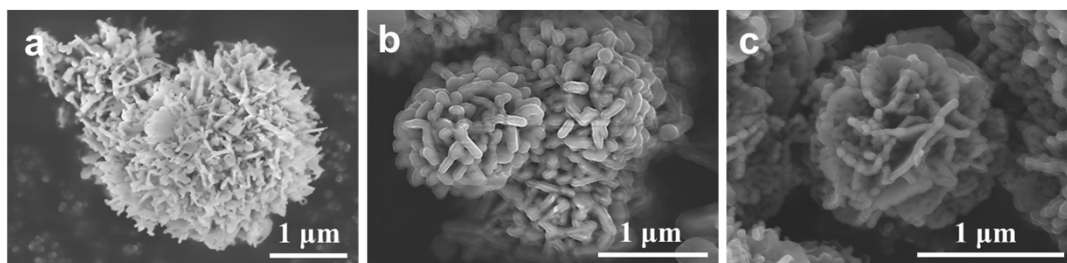
Fig. S2. SEM images of (a) Ni$_3$(BO$_3$)$_2$, (b) Ni$_3$(BO$_3$)$_2$@PDA, and (c) Ni$_3$(BO$_3$)$_2$/NC samples.
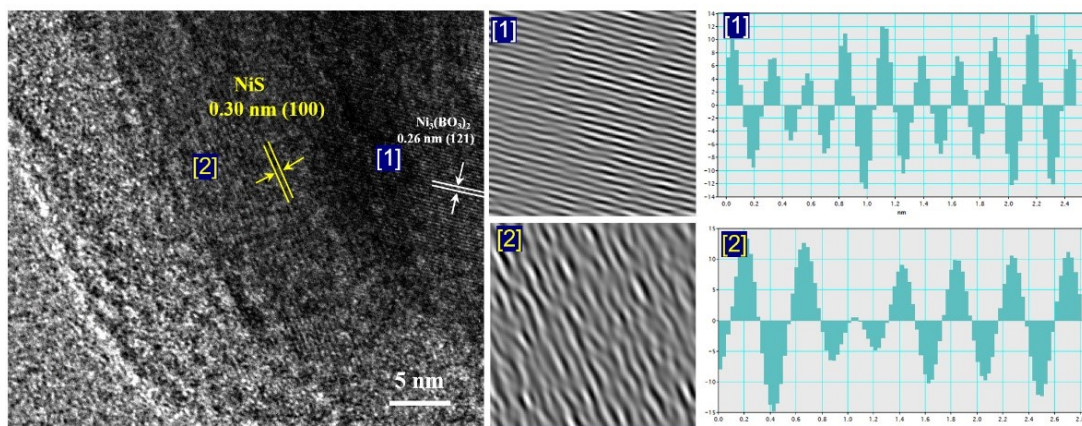
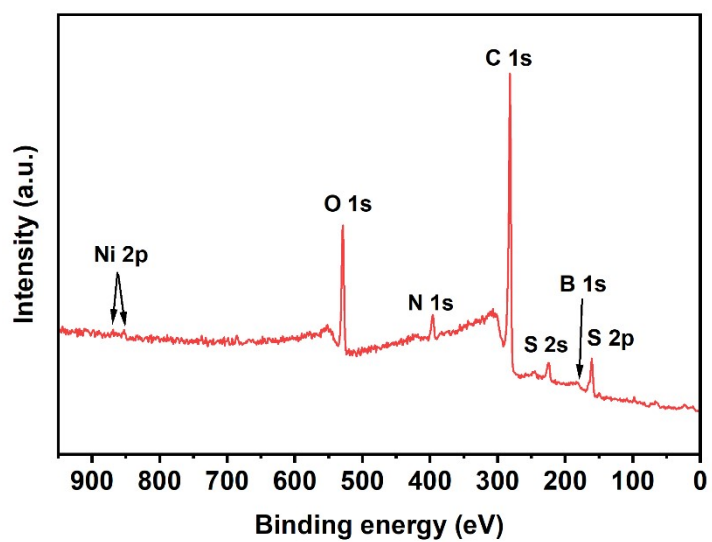**Fig. S3** HRTEM images of NiS/Ni₃(BO₃)₂/NC.

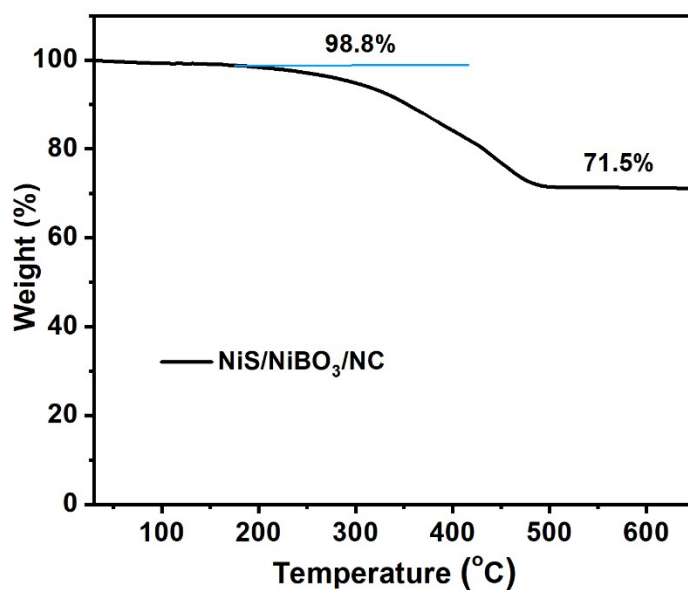

Fig. S4 XPS spectrum of NiS/Ni₃(BO₃)₂/NC survey scan.

Fig. S5 TGA curve of NiS/Ni$_3$(BO$_3$)$_2$/NC in air.

Based on XPS analysis of the NiS/Ni$_3$(BO$_3$)$_2$/NC sample, the atomic ratio of O and S is 2.26:1. Therefore, the molar ratio of NiBO$_3$: NiS is 1.5:1. Assuming the mass fractions of NiS, NiBO$_3$, and NC are x, y, and z, we can obtain the following equation:

$$x + y + z = 1.0$$

$$y : x = 1.95$$

$$0.18x + z = 0.265$$

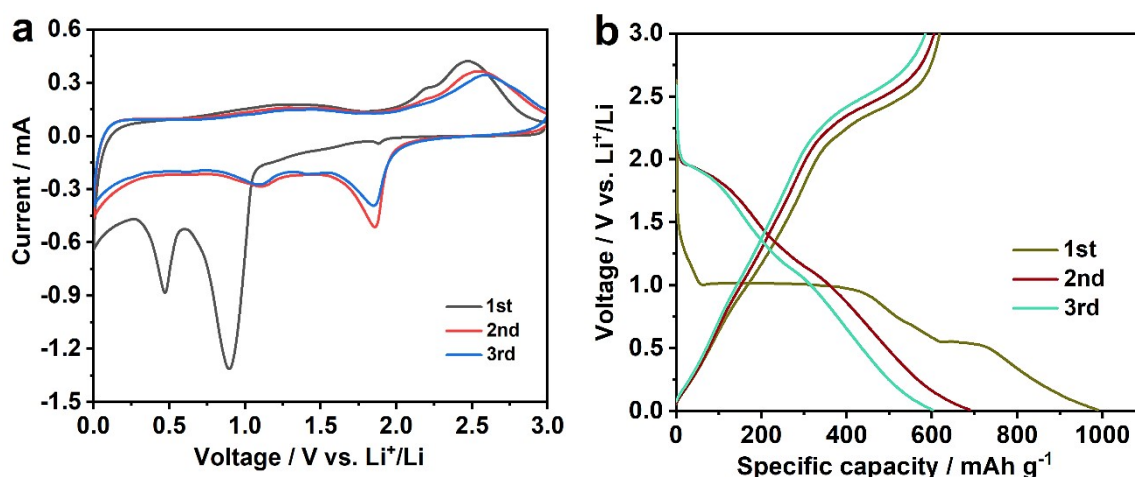Then, x = 26.5%, y = 51.7%, z = 21.8%.

Fig. S6 CV curves and GDC profiles of $Ni_3(BO_3)_2$/NC anode for LIBs.

Fig. S6a presents CV cycles of the $Ni_3(BO_3)_2$/NC electrode at a sweep rate of 0.2 mV s^{-1}. In the cathodic initial scan process, three visible peaks are located at approximately 1.87, 0.9, and 0.47 V. The reduction peaks at 1.87 and 0.9 V can be ascribed to the insertion of lithium ions into the $Ni_3(BO_3)_2$ interlayer or defect sites to form $Li_xNi_3(BO_3)_2$ (x < 6), and the latter is associated with further reduction of $Li_xNi_3(BO_3)_2$ to Li_2O, B_2O_3 and metallic Ni nanoparticles [1, 2]. A reduction peak at 0.47 V is attributed to the formation of a solid electrolyte interphase (SEI) layer, which disappears in the subsequent cycles. During the second and third scans, the main reduction peak of 0.9 V moves to approximately 1.05 V, which may be attributed to the drastic lithium-driven, structural, or textural modified modifications [3, 4]. In the reverse anodic scan, all CV cycles revealed two oxidation peaks at around 1.28 and 2.57 V, which can be associated with the partial decomposition of the SEI films and the reversible oxidation of Ni, respectively.
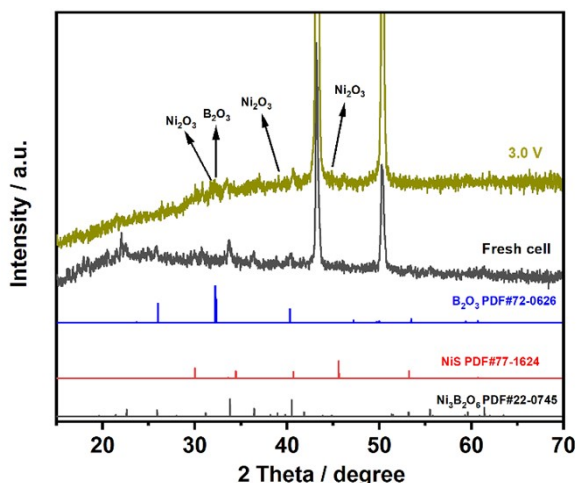
Fig. S7 (a) Ex situ XRD patterns of the NiS/Ni$_3$(BO$_3$)$_2$/NC anode during the first charge-discharge process in LIBs
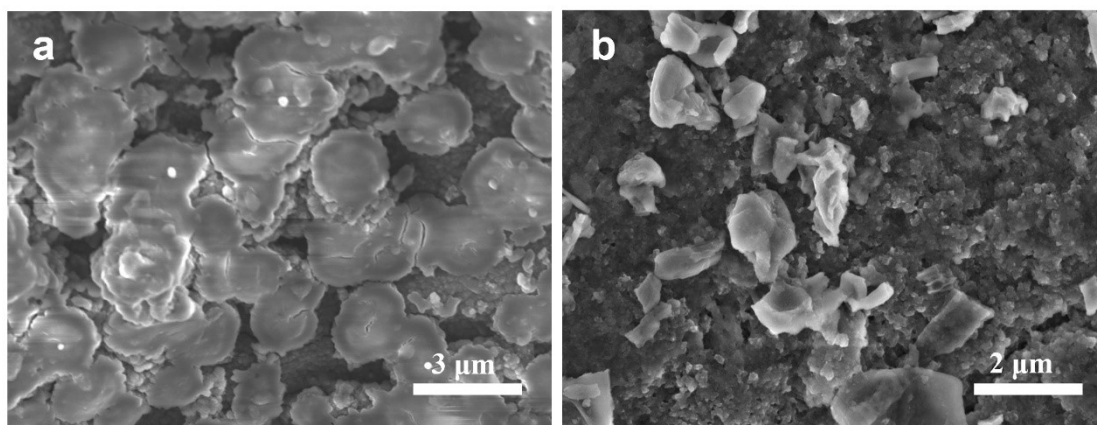

Fig. S8 SEM images of NiS/Ni$_3$(BO$_3$)$_2$/NC (a) and Ni$_3$(BO$_3$)$_2$ (b) samples after 100 cycles at 0.2 A g^{-1}, respectively.

References

1. Débart, A.; Revel, B.; Dupont, L.; Montagne, L.; Leriche, J. B.; Touboul, M.; Tarascon, J. M., Study of the Reactivity Mechanism of M$_3$B$_2$O$_6$ (with M = Co, Ni, and Cu) toward Lithium. *Chemistry of Materials* **2003,** *15* (19), 3683-3691.

2. Yi, H.; Xu, P.; Shi, G.; Xiong, Z.; Wang, R.; Shen, J.; Wang, B., The manganese oxyborate Mn$_3$(BO$_3$)$_2$ as a high-performance anode for lithium-ion batteries. *Solid State Ionics* **2022,** *380*, 115935.

3. Sun, X.; Yan, C.; Chen, Y.; Si, W.; Deng, J.; Oswald, S.; Liu, L.; Schmidt, O. G., Three-Dimensionally "Curved" NiO Nanomembranes as Ultrahigh Rate Capability Anodes for Li-Ion Batteries with Long Cycle Lifetimes. *Advanced Energy Materials* **2014,** *4* (4), 1300912.

4. Wang, B.; Wang, G.; Cheng, X.; Wang, H., Synthesis and electrochemical investigation of core-shell ultrathin NiO nanosheets grown on hollow carbon microspheres composite for high performance lithium and sodium ion batteries. *Chemical Engineering Journal* **2016,** *306*, 1193-1202.